



Article

# DNA Methylation Signature for *JARID2*-Neurodevelopmental Syndrome

Eline A. Verberne<sup>1,†</sup>, Liselot van der Laan<sup>1,†</sup> , Sadegheh Haghshenas<sup>2</sup>, Kathleen Rooney<sup>2,3</sup> , Michael A. Levy<sup>3</sup>, Mariëlle Alders<sup>1</sup>, Saskia M. Maas<sup>1</sup>, Sandra Jansen<sup>1</sup>, Agne Lieden<sup>4,5</sup>, Britt-Marie Anderlid<sup>4,5</sup>, Louise Rafael-Croes<sup>6</sup>, Philippe M. Campeau<sup>7</sup>, Ayeshah Chaudhry<sup>8,9</sup>, David A. Koolen<sup>10</sup> , Rolph Pfundt<sup>10</sup>, Anna C. E. Hurst<sup>11</sup> , Frederic Tran-Mau-Them<sup>12,13</sup>, Ange-Line Bruel<sup>12,13</sup>, Laetitia Lambert<sup>14</sup>, Bertrand Isidor<sup>15</sup>, Marcel M. A. M. Mannens<sup>1</sup>, Bekim Sadikovic<sup>2,3,\*</sup>, Peter Henneman<sup>1,\*</sup> and Mieke M. van Haelst<sup>1,‡</sup>

- <sup>1</sup> Department of Human Genetics, Amsterdam Reproduction & Development Research Institute, Amsterdam University Medical Centers, Meibergdreef 9, 1105 AZ Amsterdam, The Netherlands; e.verberne@amsterdamumc.nl (E.A.V.); l.vanderlaan@amsterdamumc.nl (L.v.d.L.); m.alders@amsterdamumc.nl (M.A.); s.m.maas@amsterdamumc.nl (S.M.M.); sandra.jansen@amsterdamumc.nl (S.J.); m.a.mannens@amsterdamumc.nl (M.M.A.M.M.); m.vanhaelst@amsterdamumc.nl (M.M.v.H.)
- <sup>2</sup> Department of Pathology and Laboratory Medicine, Western University, London, ON N6A 3K7, Canada; seyyedehsadegheh.haghshenas@lhsc.on.ca (S.H.); kathleen.rooney@lhsc.on.ca (K.R.)
- <sup>3</sup> Verspeeten Clinical Genome Centre, London Health Sciences Centre, London, ON N6A 5W9, Canada; michael.levy@lhsc.on.ca
- <sup>4</sup> Department of Clinical Genetics, Karolinska University Hospital, 17176 Stockholm, Sweden; agne.lieden@ki.se (A.L.); britt.marie.anderlid@ki.se (B.-M.A.)
- <sup>5</sup> Department of Molecular Medicine and Surgery, Karolinska Institutet, 17176 Stockholm, Sweden
- <sup>6</sup> Department of Pediatrics, Dr. Horacio E. Oduber Hospital, Dr. Horacio E. Oduber Boulevard 1, Oranjestad, Aruba; l.rafael@hoharuba.com
- <sup>7</sup> Department of Pediatrics, University of Montreal, Montreal, QC H4A 3J1, Canada; p.campeau@umontreal.ca
- <sup>8</sup> Department of Laboratory Medicine and Genetics, Trillium Health Partners, Mississauga, ON L5B 1B8, Canada; ayeshah.chaudhry@thp.ca
- <sup>9</sup> Department of Laboratory Medicine and Pathobiology, University of Toronto, Toronto, ON M5S 1A8, Canada
- <sup>10</sup> Department of Hum Genet, Radboud Institute for Molecular Life Sciences and Donders Institute for Brain, Cognition and Behaviour, Radboud University Medical Center, 6525 GA Nijmegen, The Netherlands; david.koolen@radboudumc.nl (D.A.K.); rolf.pfundt@radboudumc.nl (R.P.)
- <sup>11</sup> Department of Genetics, University of Alabama at Birmingham, Birmingham, AL 35294, USA; acehurst@uab.edu
- <sup>12</sup> UF6254 Innovation en Diagnostique Genomique des Maladies Rares, 21070 Dijon, France; frederic.tran-mau-them@u-bourgogne.fr (F.T.-M.-T.); ange-line.brue@u-bourgogne.fr (A.-L.B.)
- <sup>13</sup> Équipe Génétique des Anomalies du Développement (GAD), CHU Dijon-Bourgogne, 21000 Dijon, France
- <sup>14</sup> Service de Génétique Clinique, CHRU Nancy, 54000 Nancy, France; l.lambert@chru-nancy.fr
- <sup>15</sup> Service de génétique médicale, CHU de Nantes, 44000 Nantes, France; bertrand.isidor@chu-nantes.fr
- \* Correspondence: bekim.sadikovic@lhsc.on.ca (B.S.); p.henneman@amsterdamumc.nl (P.H.)
- † These authors contributed equally to this work.
- ‡ These authors contributed equally to this work.



**Citation:** Verberne, E.A.; van der Laan, L.; Haghshenas, S.; Rooney, K.; Levy, M.A.; Alders, M.; Maas, S.M.; Jansen, S.; Lieden, A.; Anderlid, B.-M.; et al. DNA Methylation Signature for *JARID2*-Neurodevelopmental Syndrome. *Int. J. Mol. Sci.* **2022**, *23*, 8001. <https://doi.org/10.3390/ijms23148001>

Academic Editor: Elena Bonora

Received: 16 June 2022

Accepted: 19 July 2022

Published: 20 July 2022

**Publisher's Note:** MDPI stays neutral with regard to jurisdictional claims in published maps and institutional affiliations.



**Copyright:** © 2022 by the authors. Licensee MDPI, Basel, Switzerland. This article is an open access article distributed under the terms and conditions of the Creative Commons Attribution (CC BY) license (<https://creativecommons.org/licenses/by/4.0/>).

**Abstract:** *JARID2* (Jumonji, AT Rich Interactive Domain 2) pathogenic variants cause a neurodevelopmental syndrome, that is characterized by developmental delay, cognitive impairment, hypotonia, autistic features, behavior abnormalities and dysmorphic facial features. *JARID2* encodes a transcriptional repressor protein that regulates the activity of various histone methyltransferase complexes. However, the molecular etiology is not fully understood, and *JARID2*-neurodevelopmental syndrome may vary in its typical clinical phenotype. In addition, the detection of variants of uncertain significance (VUSs) often results in a delay of final diagnosis which could hamper the appropriate care. In this study we aim to detect a specific and sensitive DNA methylation signature for *JARID2*-neurodevelopmental syndrome. Peripheral blood DNA methylation profiles from 56 control subjects, 8 patients with (likely) pathogenic *JARID2* variants and 3 patients with *JARID2* VUSs were analyzed. DNA methylation analysis indicated a clear and robust separation between patients with (likely) pathogenic variants and controls. A binary model capable of classifying patients with the *JARID2*-neurodevelopmental syndrome was constructed on the basis of the identified epismature. Patients

carrying VUSs clustered with the control group. We identified a distinct DNA methylation signature associated with *JARID2*-neurodevelopmental syndrome, establishing its utility as a biomarker for this syndrome and expanding the EpiSign diagnostic test.

**Keywords:** *JARID2*; developmental disorder; DNA methylation; epigenetics; episignature

## 1. Introduction

*JARID2* (Jumonji, AT Rich Interactive Domain 2; OMIM 601594) haploinsufficiency has been associated with a clinically distinct neurodevelopmental syndrome [1–3]. It is characterized by developmental delay, cognitive impairment (ranging from borderline intellectual functioning to severe intellectual disability), hypotonia, autistic features and behavior abnormalities. Dysmorphic facial features include high anterior hairline, broad forehead, deeply set eyes, infraorbital dark circles, depressed nasal bridge, bulbous nasal tip and full lips.

*JARID2* encodes a transcriptional repressor protein that regulates the activity of various histone methyltransferase complexes. The *JARID2* protein plays a role in the recruitment and activation of the polycomb repressive complex 2 (PRC2), which suppresses expression of target genes through histone H3 lysine 27 (H3K27) methylation [4,5]. In addition, it has been shown in mice that *Jarid2* regulates *Notch1* expression during cardiac development through recruitment of *Setdb1*, resulting in increased methylation of histone H3 lysine 9 [6]. Because of its function in epigenetic regulation, we hypothesize that *JARID2* aberrations manifest with a specific DNA methylation (DNAm) pattern. It has been demonstrated previously that disorder-specific DNAm patterns across the genome (episignatures) can be detected through EpiSign analysis [7]. With this test, 57 episignatures associated with 65 genetic syndromes can be currently detected, including ADNP syndrome, CHARGE syndrome, Down syndrome, Kleefstra syndrome 1 and Kabuki syndrome 1 and 2 [8]. Most of the episignatures previously discovered involve genes that are part of the epigenetic machinery described by Bjornsson [9].

An important, and currently applied, clinical utility of DNAm signatures involves the reclassification of previously identified variants of unknown significance (VUS) in genes linked to rare genetic disorders [10]. In addition, DNAm signatures can be used as a diagnostic tool in patients with a suspected genetic disorder and molecularly unconfirmed diagnosis [11]. Apart from these diagnostic purposes, DNAm analysis can provide insights into the molecular mechanisms underlying genetic disorders.

In this study, we aim to (1) detect a DNAm signature for the *JARID2*-neurodevelopmental syndrome using eight patients with (likely) pathogenic *JARID2* variants and (2) assess pathogenicity of three *JARID2* VUSs with the established DNAm signature.

## 2. Results

### 2.1. Identification and Assessment of an Episignature for the *JARID2*-Neurodevelopmental Syndrome

The clinical and molecular details of our patient cohort are summarized in Table 1 and Figure 1.

**Table 1.** Patients' clinical and genetic characteristics. Patient 7 is the mother of patient 6. Patient 9 and 11 are not related.

Patient #	1	2	3	4	5	6	7	8	9	10	11
<b>Variant</b>	(15291644_15388348)x1	(15330889_15419256)x1	(15374392_15405436)x1	c.2866dupGp.(Glu956-GlyfsTer72)	c.2731 + 1G > C	(15383717_15462037)x1	(15383717_15462037)x1	deletion exons 6-18 *	c.2363G > Ap.(Arg788Gln)	c.1930G > Ap.(Glu644Lys)	c.2363G > Ap.(Arg788Gln)
<b>Genomic position (hg19)</b>	-	-	-	(15511546dup)	(15507648G > C)	-	-	-	(15501555G > A)	(15497386G > A)	(15501555G > A)
<b>Variant type</b>	Del	Del	Del	FS	SS	Del	Del	Del	Mis	Mis	Mis
<b>Inheritance</b>	dn	dn	dn	dn	dn	mat	NA	dn	dn	dn	mat †
<b>Classification</b>	P	P	P	P	LP	P	P	P	VUS	VUS	VUS
<b>Gender</b>	M	F	F	M	M	F	F	M	F	M	M
<b>Age (years)</b>	14	21	18	14	5	6	36	9	43	12	8
<b>Intellectual functioning</b>	Mild ID (IQ 61-74)	Borderline intellectual functioning (IQ 82)	Mild ID (IQ 50)	Moderate ID(IQ NA)	IQ NA	Normal	Learning difficulties (IQ NA)	Mild ID (IQ NA)	Learning difficulties (IQ 79)	Mild ID (IQ 66)	Normal
<b>Developmental delay</b>	+	+	+	+	+	+	+	+	+	+	+
<b>Behavior abnormalities</b>	-	+	-	+	-	-	-	+	+	-	-
<b>Autistic features</b>	+	-	+	+	-	-	-	+	+	-	-
<b>ASD diagnosis</b>	-	-	-	+	-	-	-	+	+	-	-
<b>Hypotonia</b>	-	-	-	-	+	-	-	+	-	-	+
<b>Gait disturbance</b>	-	-	-	-	-	+	-	+	-	-	+
<b>MRI abnormalities</b>	NA	NA	NA	Small posterior fossa cyst or mega cisterna magna	Arachnoid cyst	NA	NA	Normal spinal cord MRI	NA	NA	Brain MRI: lack of myelination. Normal spinal MRI.

Table 1. Cont.

Patient #	1	2	3	4	5	6	7	8	9	10	11
<b>Dysmorphic features</b>											
- Broad forehead	+	-	-	-	+	-	-	+	-	-	+
- High anterior hair line	-	+	+	+	-	+	-	+	-	-	+
- Prominent supraorbital ridges	-	-	-	-	-	-	-	+	-	-	-
- Deeply set eyes	-	+	+	-	+	-	-	+	-	-	+
- Infraorbital dark circles	+	-	+	-	-	+	-	+	-	-	+
- Midface hypoplasia	-	+	-	-	-	-	-	-	-	-	+
- Depressed nasal bridge	-	-	+	-	-	-	-	slight	-	-	-
- Bulbous nasal tip	-	-	+	-	-	+	+	-	-	-	+
- Short philtrum	-	+	+	+	-	-	-	-	-	-	+
- Full lips	-	-	+	+	-	-	-	-	-	-	+
<b>Other anomalies</b>	Pes plano valgus, mild hypermetropia	Submucous cleft palate, bifid uvula	Fetal finger pads, slight tapering of digit II and V bilateral.	2 café au lait macules	Right cryptorchidism, congenital torticollis	Supernumerary tooth	-	Kyphoscoliosis, bladder spasticity	Strabismus convergens, camptodactyly digiti V of the hands, syndactyly dig 2–3 of the feet		Severe global spasticity, neurogenic bladder

Variants based on NM\_004973.4. Del; Deletion, FS; Frameshift, SS; Splice site, Mis; missense, dn; de novo, mat; maternal, LP; likely pathogenic, P; pathogenic, VUS; variant of unknown significance, F; Female, M; Male, ID; intellectual disability, ASD; autism spectrum disorder, NA; not assessed, -; absent, +; present. Patient 1, 2, 3, 4, 6 and 7 are analyzed with array techniques and the notation arr[GRCH37]6p22.3 is used. \* Exact position is not known. † Mother apparently unaffected.

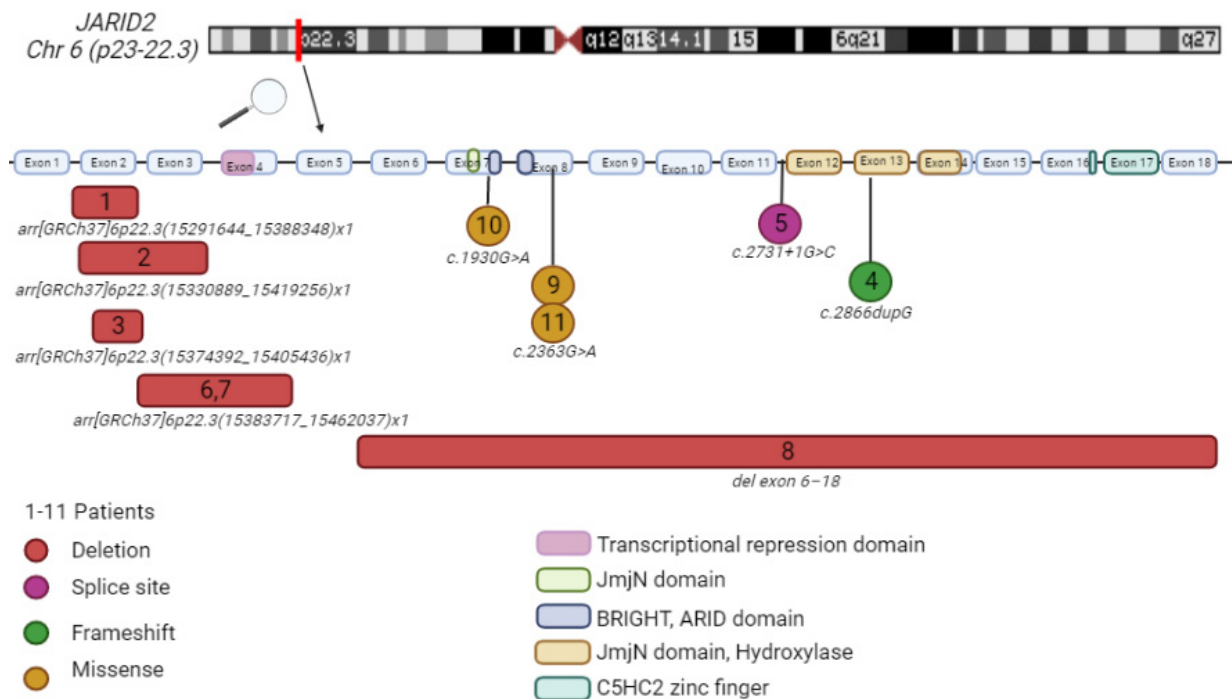


**Figure 1.** Patients' genetic information. The numbers match with the numbers in the table and figures. Comparison between the patients with deletions (red square), splice site (purple circle), frameshift (green circle) and missense (yellow circle) variants. Patients 6 and 7 have the same deletion and are related (mother and daughter). Patient 9 and 11 are not related to each other. Alamut Visual version NM\_004973.4 *JARID2*. Created with BioRender.com [1,5].

All samples within this study passed our quality control and the clean dataset involved 776314 probes. Our three-step feature selection procedure yielded 150 probes (Tables S1 and S2) with which we observed a clear clustering of patients and controls, based on hierarchical clustering and MDS visualizations. More detailed information about the selected probes is given in Table S1. The methylation levels ( $\beta$  values) at those probes for Patients 1–8 and for the control samples have also been provided in Table S2. Both of the unsupervised models indicated the presence of a robust epesignature (Figure 2).

The methylation pattern of patient samples carrying *JARID2* missense VUSs (patients 9–11) were also evaluated by plotting them alongside patients with a (likely) pathogenic variant and control individuals, using the selected probes. The three *JARID2* case samples carrying VUSs clustered with the control individuals (Figure 3).

In order to assess the reproducibility of the epesignature, eight rounds of “leave one out” cross-validation were performed. At each iteration, seven case samples and the matched control samples were used for probe selection, and subsequently, using the selected probes, those samples were plotted alongside the sample that was not used for probe selection, using an MDS. All testing samples clustered with the remaining case samples (Figure 4).

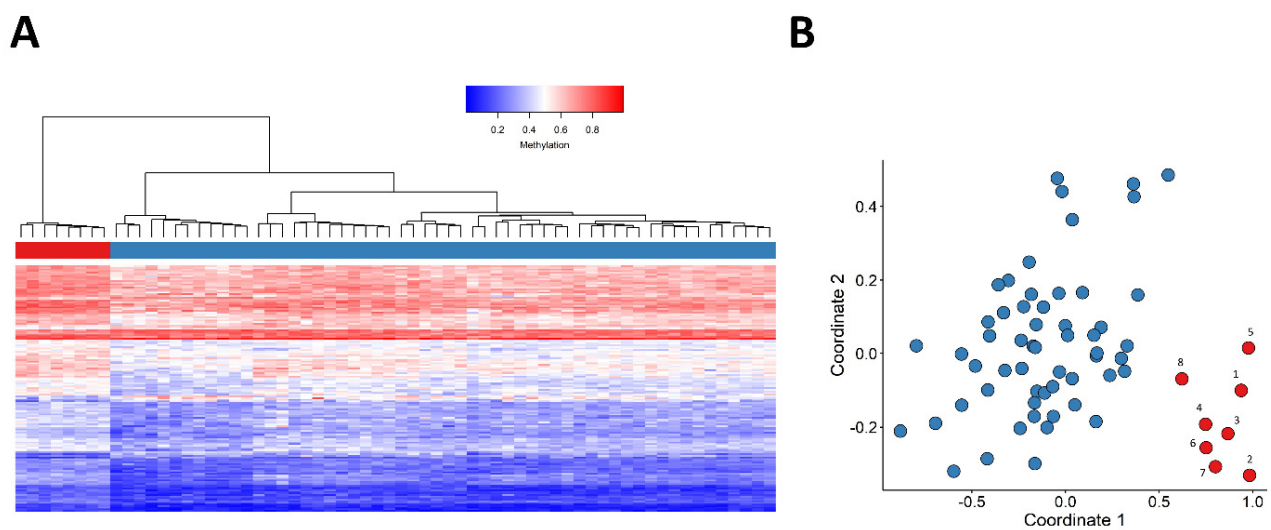


**Figure 2.** Assessment of the robustness of the *JARID2*-neurodevelopmental syndrome epigenature in distinguishing between the case and control groups using unsupervised models. **(A)** Hierarchical clustering model, wherein rows represent probes and columns represent individual samples. Patients and control samples are depicted with red and blue, respectively. Heatmap gradient colors scale illustrates methylation levels ranging from blue (no methylation) to red (full methylation). **(B)** Visualization of robust segregation of patients and controls by multidimensional scaling (MDS); X-axis represents coordinate 1 and Y-axis represents coordinate 2 and red and blue circles represent case and control samples, respectively. Patients and control samples (depicted in red and blue, respectively) clearly cluster separately.

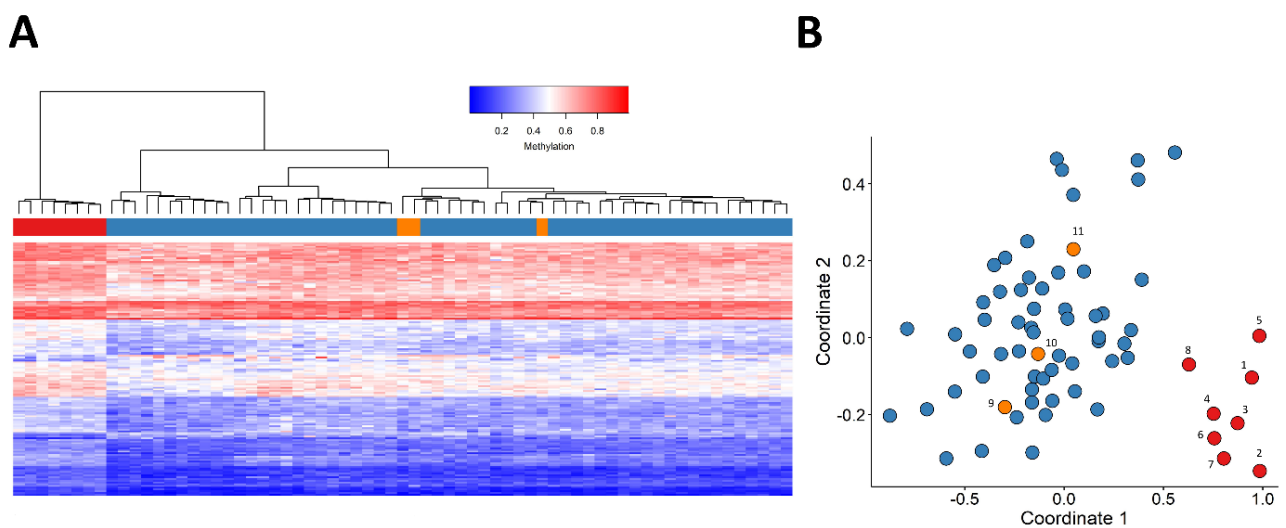


**Figure 3.** Adding patients 9–11 as a testing sample to the unsupervised clustering models. In both figures, individuals depicted in red (patients 1–8) and blue (control samples) were used for feature selection, and individuals indicated with orange (patients 9–11) were not used for selecting probes. **(A)** Hierarchical clustering, **(B)** Multidimensional scaling (MDS) plot, X-axis represents coordinate 1 and Y-axis represents coordinate 2. Patients and control samples (depicted in red and blue, respectively) clearly cluster separately. The samples with *JARID2* VUS (orange) clustered together with controls.

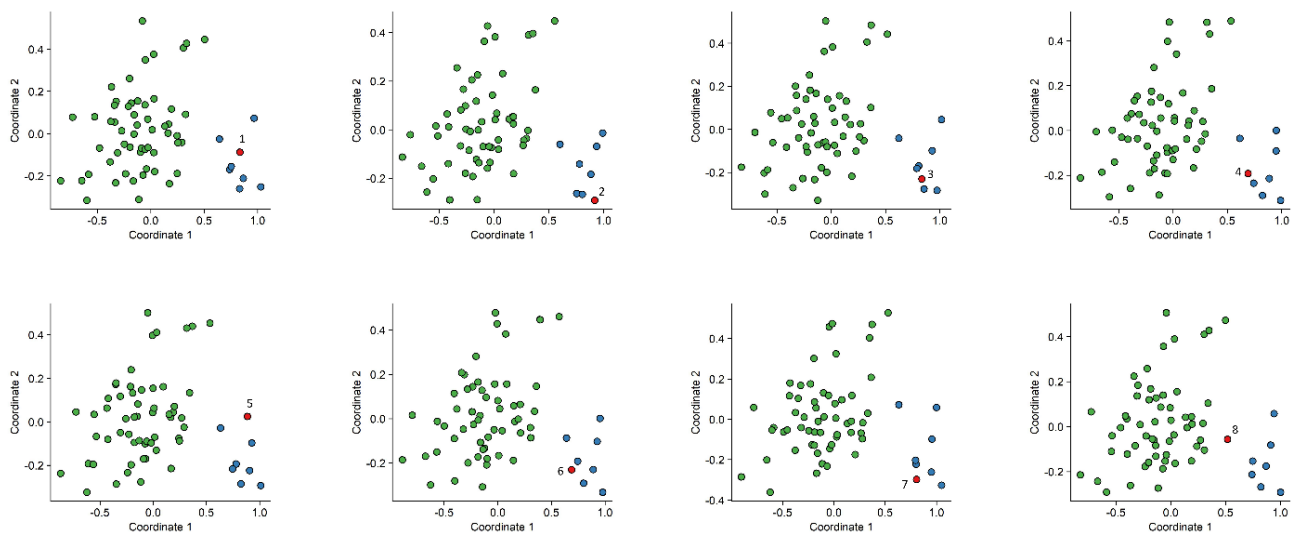


**Figure 4.** Multidimensional scaling (MDS) plots generated after eight rounds of “leave one out” cross-validation. X-axis represents coordinate 1 and Y-axis represents coordinate 2, leaving one case sample for testing (annotated in red) at each round. Control samples are annotated in green and patient samples annotated in blue. Robust clustering of the test patient with discovery patients was observed.

### 2.2. Construction of a Classification Model

In order to ensure accurate classification of *JARID2*-neurodevelopmental syndrome patients, a support vector machine (SVM) classifier was constructed using the selected set of probes. The SVM generates a methylation variant pathogenicity (MVP) score for each individual, ranging between 0–1. Higher scores indicate more similarity to the identified *JARID2*-neurodevelopmental epismature. The SVM classifier has a default cut-off of 0.5 for the MVP score to predict the class. The classifier was constructed by training the 8 case samples with (likely) pathogenic *JARID2* variants against the 56 matched control samples (used for probe selection), 75% of other control samples, and 75% of case samples from 57 other rare genetic disorders. The remaining 25% were used for testing the model. All the samples with (likely) pathogenic *JARID2* variants received MVP scores near 1, while all the control samples and case samples from other neurodevelopmental disorders received low MVP scores. Therefore, we conclude that our model has full sensitivity and specificity. The three patients with *JARID2* VUSs were also supplied into the model and received MVP scores near zero, indicating the dissimilarity of their methylation profile to the identified *JARID2*-neurodevelopmental syndrome epismature (Figure 5).

### 2.3. Differentially Methylated Regions and Gene Set Enrichment Analysis

Using the DMRcate algorithm [12] with 5% mean methylation difference and a minimum of three CpGs, no significant DMRs were detected. Additional exploration of the set of 150 selected probes yielded in total seven regions involving two or three probes with a consistent direction of effect.

### 2.4. Gene Set Enrichment Analysis

Using the different gene set enrichments web tools and distinct databases did not yield consistent associated molecular pathways.

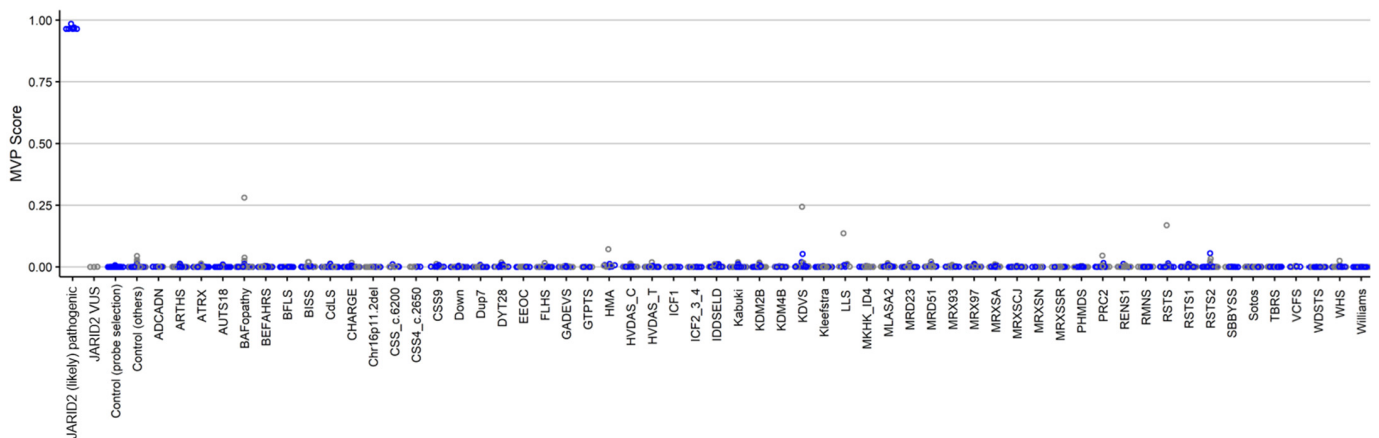


**Figure 5.** MVP scores generated by the support vector machine (SVM) classification model. All of the case samples (*JARID2* (likely) pathogenic) received high MVP scores, in contrast to the control samples and individuals from all the other disorders that received low scores, indicating the full specificity of the model. The three samples with *JARID2* VUSs yielded scores near zero.

### 3. Discussion

Generally established during embryonic development, DNAm patterns are usually detectable in peripheral blood, making them easily accessible biomarkers for use in a clinical setting [13]. DNAm epigenatures have recently been used for helping to provide a more definitive diagnosis for patients with Mendelian neurodevelopmental disorders, especially the unresolved cases, as well as to reclassify VUSs [10,14–17].

In this study, we were able to detect a specific DNAm signature for *JARID2*-neurodevelopmental syndrome in a cohort of eight patients with (likely) pathogenic *JARID2* variants. Hierarchical clustering and MDS visualization showed a clear distinction between patients and controls, indicating robustness of the epigenature. In order to assess the reproducibility of the epigenature, we performed eight rounds of cross-validation. Each round, the testing sample clustered together with the patient samples, indicating that it is a reproducible epigenature. In addition, our SVM classification model showed that the methylation signature was highly sensitive and specific for the *JARID2*-neurodevelopmental syndrome and not sensitive to other diseases that are linked to the epigenetic machinery and also associated with features such as developmental delay and intellectual disability.

The established *JARID2*-neurodevelopmental syndrome epigenature was then utilized to assess the pathogenicity of the two missense variants in *JARID2*, identified in patients 9–11. These three patients clustered with the control individuals in the MDS plot and yielded MVP scores near zero, indicating their different methylation profile from that of the 8 patients with (likely) pathogenic *JARID2* variants. As epigenatures may only be used to upgrade a VUS to (likely) pathogenic if the related epigenature is present, these negative results do not rule out pathogenicity [18]. For example, it might be possible that *JARID2* missense variants are associated with a distinct epigenature. In ADNP syndrome, for instance, two distinct epigenatures have been identified, as a result of truncating variants in two distinct protein domains of the *ADNP* gene [17]. However, since clinical features of the three patients with a *JARID2* VUS are not highly specific to only *JARID2*-neurodevelopmental syndrome, we think that these *JARID2* missense variants might very well be benign variants and that the phenotype of these patients is caused by another, currently unknown, genetic aberration. This is further supported by the observation that patients 9 and 10 did not show the facial dysmorphisms that have been associated with *JARID2*-neurodevelopmental syndrome. The phenotype of patient 11 included severe global spasticity and lack of myelination on brain MRI, both not known to be associated with *JARID2*-neurodevelopmental syndrome at present. In addition, the missense variant c.2363G > A p.(Arg788Gln) that was identified in patients 9 and 11 is not located in any of the currently known domains that are important for functioning. Moreover, the amino acid



change from arginine to glutamine is predicted to lead to a normal functioning protein [19]. The missense variant c.1930G > A p.(Glu644Lys) that was identified in patient 10 is located in the BRIGHT, ARID domain (AT-rich interaction). This domain plays an important role in developmental, tissue-specific gene expression and proliferation control and it can potentially bind DNA [20,21]. However, the amino acid change from glutamate to lysine is predicted to lead to a normal functioning protein [19]. No other possible disease-causing variants were identified by whole exome sequencing in these three patients, although patient 9 carried two de novo VUSs in the *TNRC18* gene, for which there are currently no known disease associations. In addition, microarray analysis was performed in patient 10, with normal results.

DMR analysis did not detect any significant *JARID2* associated region. However, when we evaluated the list of 150 selected probes, we observed seven regions that involved >2 selected probes, which were located in direct vicinity of each other and showed a consistent direction of effect. Five out of these seven regions were annotated to genes of which the function remains unclear in relation to the *JARID2* disease phenotype. However, two of these seven regions were annotated to genes previously linked with aberrant neurological development. First, the *NLGN2* gene previously was associated with autism and pervasive developmental disorders [22]. Secondly, the *ADGRL2* (*LPHN2*) gene was previously associated with a mild brain malformation (rhombencephalosynapsis) [23]. Detailed follow-up studies are needed to explore whether these association indeed play a role in disease or intellectual deficit at a functional level. Further exploration of the 150 selected probes using different gene set enrichment web tools and distinct databases did not yield consistent associated molecular pathways. However, we did detect enrichment of genes annotated to the endochondral ossification pathway (Webgestalt, Wikipathway). Whether the latter truly is related to particular dysmorphic features of the *JARID2* disease phenotype remains, however, unclear and needs further in-depth translational research. However, regardless of the underlying biology, the clear association between the detected DNA methylation signature and the *JARID2*-neurodevelopmental syndrome establishes its utility in diagnostic testing for *JARID2*-neurodevelopmental syndrome.

A possible limitation of this study is the relatively small sample size of eight patients. However, considering the rarity of Mendelian neurodevelopmental disorders, episignatures are identified, using as few as five patients [8]. The availability of more samples in the future may facilitate the identification of more sensitive and specific episignature for the *JARID2*-neurodevelopmental syndrome.

## 4. Materials and Methods

### 4.1. Subjects and Study Cohort

The patient cohort included a total of eleven individuals (six males and five females) with variants in *JARID2*, of which seven (patient 1–5, 9 and 10) have been previously described in the literature [1]. All patients were identified in a clinical diagnostic setting. The *JARID2* variants had been identified through microarray analysis, whole exome sequencing or an autism/intellectual disability gene panel and were classified according to the guidelines of the American College of Medical Genetics (ACMG) [24]. Eight patients carried a pathogenic or likely pathogenic variant, including six patients with a deletion of at least one exon of *JARID2*, one patient with a frameshift variant and one with a splice site variant. Three patients carried a VUSs in the *JARID2* gene; all three were missense variants. Since haploinsufficiency of *JARID2* has been identified as the disease mechanism in *JARID2*-neurodevelopmental syndrome [1,2], the eight patients carrying a (likely) pathogenic *JARID2* variant were used for the discovery phase, i.e., episignature detection. Subsequently, the established episignature was used to further assess pathogenicity of the three missense variants. We selected 56 control samples from the EpiSign Knowledge Database (EKD), <https://episign.lhsc.on.ca/index.html>, matched by age, sex and array type. EKD is a database consisting of more than 600 healthy control samples and above 1000 individuals from 57 neurodevelopmental disorders with a known episignature. The

samples in the EKD include samples that were processed in the same batches as those from the study cohort at AUMC and were then sent to LHSC for methylation analysis. Control samples were all selected from the same batches as our *JARID2* case samples, and none of them had a *JARID2* variant or a clinical diagnosis of *JARID2*-neurodevelopmental syndrome. The age of control individuals ranged from 2 to 50 years, with a mean of 20.1 years and a median of 10 years. In total, 46% percent of them were females and 54% males. The control to case ratio was increased until the matching quality reached an optimum point, meaning that the case and control cohorts have the highest similarity with regard to their age, sex and array type. This resulted in a control to case ratio of 7:1 [10].

#### 4.2. DNA Isolation and Methylation Analysis

Peripheral blood DNA was obtained according to standard techniques. DNA methylation analysis of the samples were performed using the Illumina Infinium methylation EPIC bead chip arrays (San Diego, CA, USA) according the manufacturer's protocol. Data analysis was performed at the Verspeeten Clinical Genome Centre at London Health Sciences, Canada. The analysis and discovery of epigenatures were carried out based on laboratory's previously published protocols [7,10,11]. In order to minimize batch effect herein, samples were randomly divided over separate batches.

#### 4.3. Quality Control of DNAm Profiles and Feature Selection

The details of the quality control and feature selection procedures were previously described in detail [25]. In brief, methylated and unmethylated signal intensities were imported into R (v 4.0.5) and normalized using background correction available under the minfi (v 1.34.0) package [26]. Probes that were annotated to the allosomes, contained single-nucleotide polymorphisms (SNPs) at or near CpG interrogation or single nucleotide extension, had detection *p*-value above 0.01 or were known to cross-react with chromosomal locations other than their target regions were eliminated from the dataset. Principal component analysis (PCA) was performed in order to detect outliers and observe the overall batch structure. Methylation level ( $\beta$ -value) for each probe was calculated as the ratio of methylated signal intensity to the sum of methylated and unmethylated signal intensities. In order to obtain homoscedasticity, these values were converted into M-values using the formula  $\log_2(\beta/(1 - \beta))$ . Next, differential methylation analysis between patients with (likely) pathogenic *JARID2* variants and controls was performed using a linear model available in the limma package (v 3.44.3). Blood cell proportions were estimated by the Houseman method [27] and included as covariates in the model matrix. The blood cell types used as covariates are CD4+ and CD8+ T-cells, natural killer cells, monocytes, granulocytes and b-cells as specified in the minfi package.

Since the Infinium EPIC bead chip array represents a high dimensional dataset (~860 K probes, raw data), we followed a three-step feature selection procedure. First, the 1000 most significant probes based on effect size and *p*-value, i.e., probes with the highest product of mean methylation differences between the case and control groups and negative of the logarithm of *p*-values, were selected. Subsequently, 250 probes with the highest areas under the receiver operating characteristic curve (AUROC) were retained. Finally, probes with a correlation higher than 0.9 within case and control groups separately were eliminated. The methylation levels at the remaining 150 probes were considered as the identifying epigenature for the *JARID2*-neurodevelopmental syndrome epigenature. In order to assess the robustness of the selected probes in distinguishing between the case and control groups we applied unsupervised models, herein, hierarchical clustering was performed using Ward's method on Euclidean distance, and multidimensional scaling (MDS) was applied by measuring of the pair-wise Euclidean distances between samples. In order to guarantee the stability and reproducibility of the epigenature, an eight-round leave-one-out cross-validation was performed: in each round, seven patient samples were used for probe selection, while the eighth patient sample was used as a testing sample. Subsequently, the corresponding MDSs were visualized.

#### 4.4. Construction of the Binary Classifier

In order to classify case and control samples more accurately, we applied the aforementioned identified probe set in a support vector machine (SVM), which was constructed using the *e1071* package, as previously described [7,10,11]. The classifier is constructed by training the 8 samples with (likely) pathogenic *JARID2* variants against the 56 matched control samples that were used for probe selection, 75% (N = 461) of other controls, and 75% (N = 939) of samples from 57 other neurodevelopmental disorders from the EKD, and the remaining 25% (N = 496) of these controls and other neurodevelopmental disorder samples were used for model testing. The model creates scores ranging 0–1 for each sample, which indicate the probability that the sample has a methylation profile similar to that of *JARID2*-neurodevelopmental syndrome. This score is called the methylation variant pathogenicity (MVP) score. By default, the SVM model uses a cut-off score of 0.5 for classifying the samples.

#### 4.5. Differentially Methylated Regions

The existence of differentially methylated regions (DMRs) was investigated using the DMRcate package [12], where regions containing at least three CpGs within 1 kb with a minimum methylation difference of 5% and a Fisher's multiple comparison *p*-value < 0.01 were considered significant. Further exploration for detection of DMRs was based on total set of 150 selected probes. Herein, DMRs were defined as including >2 differentially methylated probes in direct vicinity and showing consistent direction effect.

#### 4.6. Geneset Enrichment Analysis

Geneset enrichment analysis was based on DAVID [28] and Webgestalt publicly available webtools [29], using KEGG and Wikipathway databases, according default parameters.

### 5. Conclusions

In this study, we identified a highly specific DNAm signature for patients with *JARID2*-neurodevelopmental syndrome. The signature can be used to assess and reclassify *JARID2* genomic variants. In addition, the *JARID2* signature can be added to the growing list of syndromes that can be confirmed by EpiSign analysis, thus further confirming the value of EpiSign as a diagnostic tool in patients with suspected genetic disorders.

**Supplementary Materials:** The following supporting information can be downloaded at: <https://www.mdpi.com/article/10.3390/ijms23148001/s1>.

**Author Contributions:** E.A.V., L.v.d.L., M.A., M.M.A.M.M., B.S., P.H. and M.M.v.H. designed the project. E.A.V., L.v.d.L., M.A., P.H. and M.M.v.H. contributed to the sample collection. E.A.V., S.M.M., S.J., A.L., B.-M.A., L.R.-C., P.M.C., A.C., D.A.K., R.P., A.C.E.H., F.T.-M.-T., L.L., A.-L.B., B.I. and M.M.v.H. contributed to the clinical assessment of participants and diagnostic laboratory investigations. L.v.d.L. and M.A. performed the laboratory experiments. B.S. oversaw the analytical and bioinformatic aspects of this study. L.v.d.L., S.H., K.R. and M.A.L. performed the bioinformatic analysis. E.A.V., L.v.d.L. and S.H. wrote the manuscript. All authors have read and agreed to the published version of the manuscript.

**Funding:** Funding for this study is provided in part by the London Health Sciences Molecular Diagnostics Development Fund and Genome Canada Genomic Applications Partnership Program awarded to BS.

**Institutional Review Board Statement:** The study was conducted in accordance with the regulations of the Western University Research Ethics Board (REB116108, and REB106302) and The Medical Ethical Committee (METC) of the Amsterdam UMC, location AMC. METC approval waived (anonymous study, further study in line with a clinical question). All patients or their caretakers were informed about this study and gave their permission to use their DNA and medical information.

**Informed Consent Statement:** We obtained written informed consent from the patients or the patients' parents to publish patients' clinical and genetic information.

**Data Availability Statement:** All data generated or analyzed during this study are available from the corresponding author on reasonable request.

**Acknowledgments:** We would like to thank the participants described in this study.

**Conflicts of Interest:** The authors declare no conflict of interest.

## Abbreviations

DNA: Deoxyribonucleic acid; DNAm: DNA methylation; MVP: methylation variant pathogenicity; METC: Medical Ethical Committee; VUS: variant of uncertain significance; ACMG: American College of Medical Genetics; EKD: EpiSign Knowledge Database; SNPs: single-nucleotide polymorphisms; PCA: principal component analysis; AUROC: areas under the receiver operating characteristic curve; MDS: multidimensional scaling; SVM: support vector machine; DMR: differentially methylated region; DMP: differentially methylated probes.

## References

1. Verberne, E.A.; Goh, S.; England, J.; van Ginkel, M.; Rafael-Croes, L.; Maas, S.; Polstra, A.; Zarate, Y.A.; Bosanko, K.A.; Pechter, K.B.; et al. JARID2 haploinsufficiency is associated with a clinically distinct neurodevelopmental syndrome. *Genet. Med.* **2021**, *23*, 374–383. [[CrossRef](#)]
2. Barøy, T.; Miscio, D.; Strømme, P.; Stray-Pedersen, A.; Holmgren, A.; Rødningen, O.K.; Blomhoff, A.; Helle, J.R.; Stormyr, A.; Tvedt, B.; et al. Haploinsufficiency of two histone modifier genes on 6p22.3, ATXN1 and JARID2, is associated with intellectual disability. *Orphanet J. Rare Dis.* **2013**, *8*, 3. [[CrossRef](#)]
3. Cadieux-Dion, M.; Farrow, E.; Thiffault, I.; Cohen, A.S.; Welsh, H.; Bartik, L.; Schwager, C.; Engleman, K.; Zhou, D.; Zhang, L.; et al. Phenotypic expansion and variable expressivity in individuals with JARID2-related intellectual disability: A case series. *Clin. Genet.* **2022**, *102*, 136–141. [[CrossRef](#)]
4. Kasinath, V.; Beck, C.; Sauer, P.; Poepsel, S.; Kosmatka, J.; Faini, M.; Toso, D.; Aebersold, R.; Nogales, E. JARID2 and AEBP2 regulate PRC2 in the presence of H2AK119ub1 and other histone modifications. *Science* **2021**, *371*, eabc3393. [[CrossRef](#)] [[PubMed](#)]
5. Pasini, D.; Cloos, P.A.; Walfridsson, J.; Olsson, L.; Bukowski, J.P.; Johansen, J.V.; Bak, M.; Tommerup, N.; Rappsilber, J.; Helin, K. JARID2 regulates binding of the Polycomb repressive complex 2 to target genes in ES cells. *Nature* **2010**, *464*, 306–310. [[CrossRef](#)] [[PubMed](#)]
6. Mysliwiec, M.R.; Carlson, C.D.; Tietjen, J.; Hung, H.; Ansari, A.Z.; Lee, Y. Jarid2 (Jumonji, AT rich interactive domain 2) regulates NOTCH1 expression via histone modification in the developing heart. *J. Biol. Chem.* **2012**, *287*, 1235–1241. [[CrossRef](#)] [[PubMed](#)]
7. Aref-Eshghi, E.; Kerkhof, J.; Pedro, V.P.; France, G.D.; Barat-Houari, M.; Ruiz-Pallares, N.; Andrau, J.C.; Lacombe, D.; Van-Gils, J.; Fergelot, P.; et al. Evaluation of DNA methylation epesignatures for diagnosis and phenotype correlations in 42 Mendelian neurodevelopmental disorders. *Am. J. Hum. Genet.* **2020**, *106*, 356–370. [[CrossRef](#)] [[PubMed](#)]
8. Levy, M.A.; McConkey, H.; Kerkhof, J.; Barat-Houari, M.; Bargiacchi, S.; Biamino, E.; Bralo, M.P.; Cappuccio, G.; Ciolfi, A.; Clarke, A.; et al. Novel diagnostic DNA methylation epesignatures expand and refine the epigenetic landscapes of Mendelian disorders. *Hum. Genet. Genom. Adv.* **2022**, *3*, 100075. [[CrossRef](#)]
9. Bjornsson, H.T. The Mendelian disorders of the epigenetic machinery. *Genome Res.* **2015**, *25*, 1473–1481. [[CrossRef](#)]
10. Aref-Eshghi, E.; Rodenhiser, D.I.; Schenkel, L.C.; Lin, H.; Skinner, C.; Ainsworth, P.; Paré, G.; Hood, R.L.; Bulman, D.E.; Kernohan, K.D.; et al. Genomic DNA Methylation Signatures Enable Concurrent Diagnosis and Clinical Genetic Variant Classification in Neurodevelopmental Syndromes. *Am. J. Hum. Genet.* **2018**, *102*, 156–174. [[CrossRef](#)]
11. Aref-Eshghi, E.; Bend, E.G.; Colaiacovo, S.; Caudle, M.; Chakrabarti, R.; Napier, M.; Brick, L.; Brady, L.; Carere, D.A.; Levy, M.A.; et al. Diagnostic Utility of Genome-wide DNA Methylation Testing in Genetically Unsolved Individuals with Suspected Hereditary Conditions. *Am. J. Hum. Genet.* **2019**, *104*, 685–700. [[CrossRef](#)]
12. Peters, T.J.; Buckley, M.J.; Statham, A.L.; Pidsley, R.; Samarasinghe, K.; Lord, R.V.; Clark, S.J.; Molloy, P.L. De novo identification of differentially methylated regions in the human genome. *Epigenetics Chromatin* **2015**, *8*, 6. [[CrossRef](#)]
13. Sadikovic, B.; Aref-Eshghi, E.; Levy, M.A.; Rodenhiser, D. DNA methylation signatures in mendelian developmental disorders as a diagnostic bridge between genotype and phenotype. *Epigenomics* **2019**, *11*, 563–575. [[CrossRef](#)]
14. Butcher, D.T.; Cytrynbaum, C.; Turinsky, A.L.; Siu, M.T.; Inbar-Feigenberg, M.; Mendoza-Londono, R.; Chitayat, D.; Walker, S.; Machado, J.; Caluseriu, O.; et al. CHARGE and Kabuki Syndromes: Gene-Specific DNA Methylation Signatures Identify Epigenetic Mechanisms Linking These Clinically Overlapping Conditions. *Am. J. Hum. Genet.* **2017**, *100*, 773–788. [[CrossRef](#)]
15. Aref-Eshghi, E.; Schenkel, L.C.; Lin, H.; Skinner, C.; Ainsworth, P.; Paré, G.; Rodenhiser, D.; Schwartz, C.; Sadikovic, B. The defining DNA methylation signature of Kabuki syndrome enables functional assessment of genetic variants of unknown clinical significance. *Epigenetics* **2017**, *12*, 923–933. [[CrossRef](#)]
16. Schenkel, L.C.; Schwartz, C.; Skinner, C.; Rodenhiser, D.I.; Ainsworth, P.J.; Pare, G.; Sadikovic, B. Clinical Validation of Fragile X Syndrome Screening by DNA Methylation Array. *J. Mol. Diagn.* **2016**, *18*, 834–841. [[CrossRef](#)]

17. Bend, E.G.; Aref-Eshghi, E.; Everman, D.B.; Rogers, R.C.; Cathey, S.S.; Prijoles, E.J.; Lyons, M.J.; Davis, H.; Clarkson, K.; Gripp, K.W.; et al. Gene domain-specific DNA methylation epesignatures highlight distinct molecular entities of ADNP syndrome. *Clin. Epigenetics* **2019**, *11*, 64. [[CrossRef](#)]
18. Sadikovic, B.; Levy, M.A.; Kerkhof, J.; Aref-Eshghi, E.; Schenkel, L.; Stuart, A.; McConkey, H.; Henneman, P.; Venema, A.; Schwartz, C.E.; et al. Clinical epigenomics: Genome-wide DNA methylation analysis for the diagnosis of Mendelian disorders. *Genet. Med.* **2021**, *23*, 1065–1074. [[CrossRef](#)]
19. Grantham, R. Amino acid difference formula to help explain protein evolution. *Science* **1974**, *185*, 862–864. [[CrossRef](#)]
20. Patsialou, A.; Wilsker, D.; Moran, E. DNA-binding properties of ARID family proteins. *Nucleic Acids Res.* **2005**, *33*, 66–80. [[CrossRef](#)]
21. Li, G.; Margueron, R.; Ku, M.; Chambon, P.; Bernstein, B.E.; Reinberg, D. Jarid2 and PRC2, partners in regulating gene expression. *Genes Dev.* **2010**, *24*, 368–380. [[CrossRef](#)]
22. Nakanishi, M.; Nomura, J.; Ji, X.; Tamada, K.; Arai, T.; Takahashi, E.; Bućan, M.; Takumi, T. Functional significance of rare neurologin 1 variants found in autism. *PLoS Genet.* **2017**, *13*, e1006940. [[CrossRef](#)]
23. Vezain, M.; Lecuyer, M.; Rubio, M.; Dupé, V.; Ratié, L.; David, V.; Pasquier, L.; Odent, S.; Coutant, S.; Tournier, I.; et al. A de novo variant in ADGRL2 suggests a novel mechanism underlying the previously undescribed association of extreme microcephaly with severely reduced sulcation and rhombencephalosynapsis. *Acta Neuropathol. Commun.* **2018**, *6*, 109. [[CrossRef](#)]
24. Richards, S.; Aziz, N.; Bale, S.; Bick, D.; Das, S.; Gastier-Foster, J.; Grody, W.W.; Hegde, M.; Lyon, E.; Spector, E.; et al. Standards and guidelines for the interpretation of sequence variants: A joint consensus recommendation of the American College of Medical Genetics and Genomics and the Association for Molecular Pathology. *Genet. Med.* **2015**, *17*, 405–424. [[CrossRef](#)]
25. Aref-Eshghi, E.; Bend, E.G.; Hood, R.L.; Schenkel, L.C.; Carere, D.A.; Chakrabarti, R.; Nagamani, S.; Cheung, S.W.; Campeau, P.M.; Prasad, C.; et al. BAFopathies' DNA methylation epi-signatures demonstrate diagnostic utility and functional continuum of Coffin-Siris and Nicolaides-Baraitser syndromes. *Nat. Commun.* **2018**, *9*, 4885. [[CrossRef](#)]
26. Aryee, M.J.; Jaffe, A.E.; Corrada-Bravo, H.; Ladd-Acosta, C.; Feinberg, A.P.; Hansen, K.D.; Irizarry, R.A. Minfi: A flexible and comprehensive Bioconductor package for the analysis of Infinium DNA methylation microarrays. *Bioinformatics* **2014**, *30*, 1363–1369. [[CrossRef](#)]
27. Houseman, E.A.; Accomando, W.P.; Koestler, D.C.; Christensen, B.C.; Marsit, C.J.; Nelson, H.H.; Wiencke, J.K.; Kelsey, K.T. DNA methylation arrays as surrogate measures of cell mixture distribution. *BMC Bioinform.* **2012**, *13*, 86. [[CrossRef](#)]
28. Huang, D.W.; Sherman, B.T.; Tan, Q.; Collins, J.R.; Alvord, W.G.; Roayaei, J.; Stephens, R.; Baseler, M.W.; Lane, H.C.; Lempicki, R.A. The DAVID Gene Functional Classification Tool: A novel biological module-centric algorithm to functionally analyze large gene lists. *Genome Biol.* **2007**, *8*, R183. [[CrossRef](#)]
29. WEB-Based Gene SeT AnaLysis Toolkit. WebGestalt (WEB-Based Gene SeT AnaLysis Toolkit). 2019. Available online: <http://www.webgestalt.org> (accessed on 1 March 2022).